Jb. Geol. B.-A.	ISSN 0016-7800	Band 134	Heft 1	S. 65–81	Wien, Mai 1991

Composition and Significance of Resedimented Amphibolite Breccias and Conglomerates (Badstub Formation) in the Carboniferous of Nötsch (Eastern Alps, Carinthia, Austria)

By KARL KRAINER & ABERRA MOGESSIE*)

With 18 Figures and 4 Tables

Carinthia
Eastern Alps
Carboniferous of Nötsch
Badstub Formation
Geochemistry
Sedimentology

Österreichische Karte 1 : 50.000
Blätter 199, 200

Contents

Zusammensetzung und Bedeutung resedimentierter Amphibolitbrekzien und -konglomerate (Badstub-Formation) im Karbon von Nötsch (Ostalpen, Kärnten, Österreich)

Zusammenfassung

Die Badstub Formation (Oberstes Visé) im Karbon von Nötsch (Ostalpen, Österreich) besteht hauptsächlich aus Breccien und Konglomeraten, die sehr reich an Amphibolitgeröllen sind. Eingeschaltet sind Sandsteine, Siltsteine und Tonschiefer. Die Sedimente sind im oberen Teil der Abfolge teilweise fossilführend, auch eine Brachiopodenschillage ist eingeschaltet. Strukturelle, texturelle und kompositionelle Merkmale weisen die Sedimente als submarine Ablagerungen aus, entstanden durch verschiedene Typen von „sediment gravity flows" auf einem proximalen Fächer oder Abhang (fan deltas, slope aprons) entlang einer aktiven Störungszone an einem passiven Plattenrand.

Haupt- und Spurenelemente weisen die Amphibolitgerölle in den grobkörnigen Sedimenten der Badstub Formation als Abkömmlinge metamorpher tholeiitischer Ozeanbodenbasalte aus. Vermutlich erfolgte die Metamorphose dieser Ozeanbodenbasalte in einer frühen Transform Fault- und Riftphase im Sinne von VAI (1979) und VAI & COCOZZA (1986) im untersten Karbon entlang einer fracture zone in einem relativ schmalen Meeresarm zwischen der Karnisch-Dinaridischen Mikroplatte und einer

*) Authors' addresses: Dr. KARL KRAINER, Institute of Geology and Paleontology, University of Innsbruck, Innrain 52, A-6020 Innsbruck; Dr. ABERRA MOGESSIE, Institute of Mineralogy and Petrology, Mining University of Leoben , A-8700 Leoben.

Ostalpinen Mikroplatte. Während einer späteren Phase wurden die metamorphen Ozeanbodenbasalte herausgehoben und abgetragen. Der Abtragungsschutt wurde auf kleinen submarinen Fächern (fan deltas, slope aprons) entlang einer aktiven Störungszone abgelagert, was zur Entstehung der an Amphibolitgeröllen sehr reichen Breccien, Konglomerate und damit vergesellschafteten Sedimente der Badstub Formation führte.

Abstract

The Upper Visean Badstub Formation in the Carboniferous of Nötsch (Eastern Alps, Austria) consists of amphibolite breccias and conglomerates with intercalated sandstones, siltstones and shales. In the upper part of the sequence these sediments contain some fossils. Structural, textural and compositional features indicate that these sediments represent submarine resedimented deposits formed by sediment gravity flows on a proximal fan or slope (fan delta, slope apron) along an active fault zone at a passive margin. Major and minor element chemistry of the amphibolite clasts of the Badstub Formation showed that the clasts represent metamorphosed tholeiitic ocean floor basalts. It is assumed that metamorphism of tholeiitic ocean floor basalts took place during an early stage of transform faulting and rifting (as proposed by VAI, 1979; VAI & COCOZZA, 1986) during Early Carboniferous along a fracture zone within a relatively narrow seaway between the Carnic-Dinaridic microplate and an East Alpine microplate. During a later stage of transform faulting and rifting these metamorphosed ocean floor basalts were uplifted and redeposited on small submarine fans ore slope aprons along an active fault zone, forming the amphibolite breccias and conglomerates of the Badstub Formation.

1. Introduction and Geological Setting

The tectonically isolated Carboniferous Sequence of Nötsch (Eastern Alps, Carinthia, Austria), extending about 9 km (E–W) and maximum 3 km (N–S) is exposed at the southern margin of the Drau Range, about 20 km W of Villach (see Fig. 1).

The Carboniferous of Nötsch is fault-bounded to the north bordering the Permian-Triassic sediments of the Drau Range, and to the south bounded by the Granite Complex of Nötsch (GCN) and Gailtal Metamorphic Complex. The E margin is poorly exposed; it is probably formed by an overthrust of Permian-Triassic sediments of the Dobratsch Massif.

The Carboniferous of Nötsch is well known for more than 150 years, especially because of the rich fauna (see summaries by TOLLMANN, 1977; SCHÖNLAUB, 1982, 1985). It comprises a sequence of coarse to fine-grained clastic sediments showing sedimentary features of deep-sea and shallow marine environments (KODSI & FLÜGEL, 1970). Intercalated is an approximately 400 m thick sequence of amphibolite breccias and conglomerates with layers of thin sand-siltstones and silty shales which locally contain fossils (Fig. 2,3).

In the literature, this sequence is known as „Badstubbreccia". Much confusion exists about the origin of these sediments, which have been interpreted very differently by various authors: as diabase (FRECH, 1894), volcanic breccia (KIESLINGER, 1956), diabase breccia (SCHÖNLAUB, 1973), tectonic breccia (ANGEL, 1932), metamorphic tholeiitic basalt (TEICH, 1982) and sedimentary breccia (FELSER, 1936; SCHÖNLAUB, 1985).

This paper is an attempt to shed some light on the origin of the „Badstubbreccia" (in this paper termed Badstub Formation), the source of the amphibolite clasts within the breccia and to point out the significance of the Badstub Formation according to geodynamic processes.

2. Petrography

Detailed field work was carried out to study the structural and textural features as well as to take detailed vertical sections through parts of the Badstub Formation. Textural and compositional data were obtained by thin section microscopy. Polished thin sections were prepared for microprobe studies. On the basis of grain-size, texture and mineral composition, different types of amphibolite clasts can be distinguished.

The dominant mineral assemblage is hornblende + plagioclase ± epidote ± chlorite ± garnet ± quartz ± ilmenite ± sphene.

The main textural types are:

1) Very fine-grained amphibolites with fine metamorphic foliation consisting of hornblende (70–80 modal-%), plagioclase (up to 25 %), ± epidote ± quartz ± oxides.
2) Non-foliated to foliated, medium to coarse-grained amphibolites, consisting of hornblende (40–80 %), plagioclase (15–38 %), epidote (in thin layers up to 60 %) ± chlorite ± quartz ± sphene.
3) Epidote-amphibolites containing up to 55 % hornblende and 40 % epidote, with small amounts of plagioclase and other accessory minerals.

3. Mineral Chemistry

3.1. Analytical Methods and Data Reduction

The compositions of the minerals (feldspar, amphibole, chlorite and epidote) were determined with an ARL-SEMQ electron microprobe with four wavelength-dispersive spectrometers at the Institute of Mineralogy and Petrography, University of Innsbruck. An attached energy dispersive system (KEVEX) was used for quick qualitative and semiquantitative analyses. The conditions for wavelength analyses were 15 Kv accelerating voltage, 0.03 μA sample current and 20 sec counting time. The matrix effects were corrected by the method of BENCE & ALBEE (1968). All minerals were subjected to several spot analyses (a minimum of 10 analyses per grain).

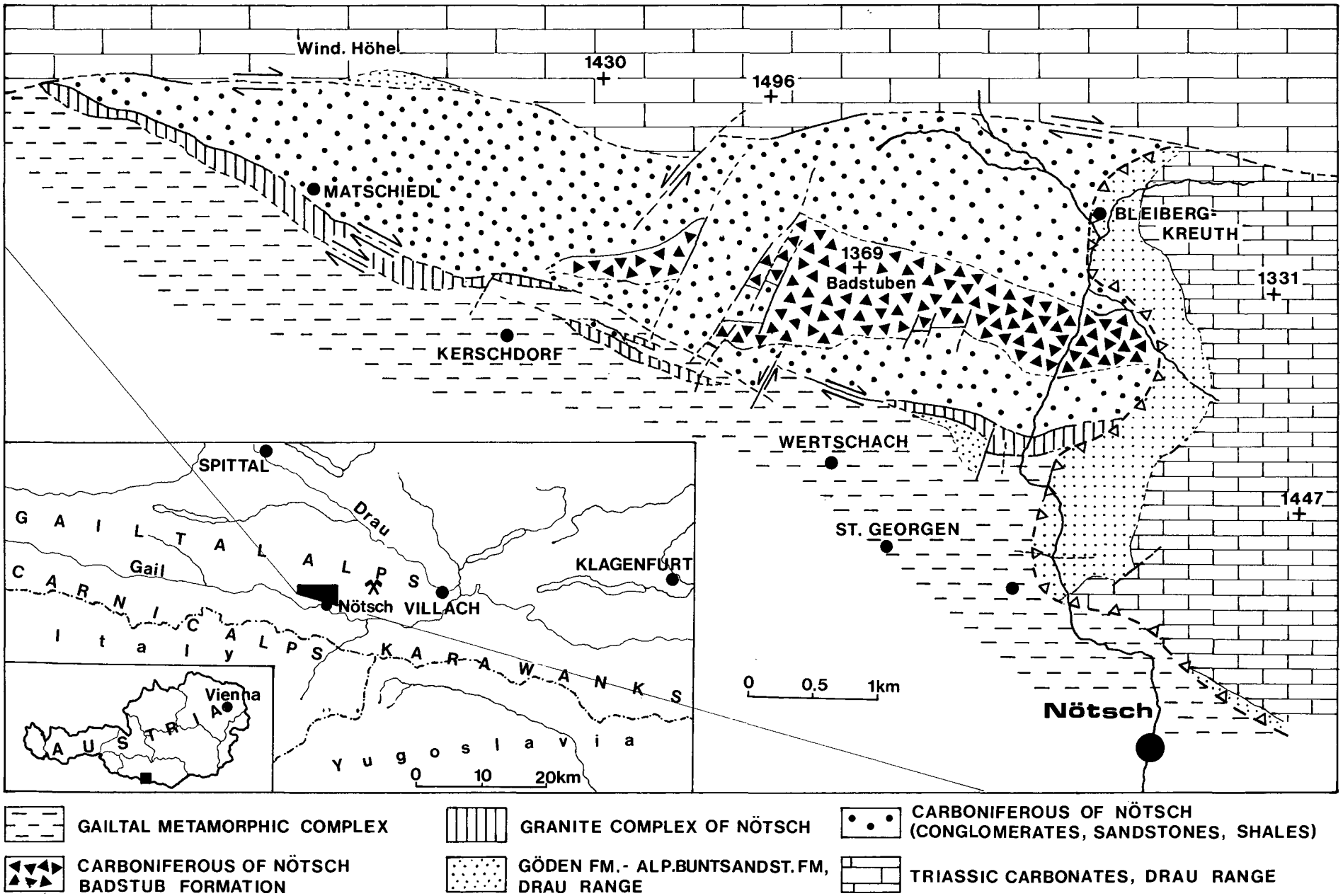

Fig. 1.
Generalized geological map of the Carboniferous of Nötsch.
Adapted from SCHÖNLAUB (1985).

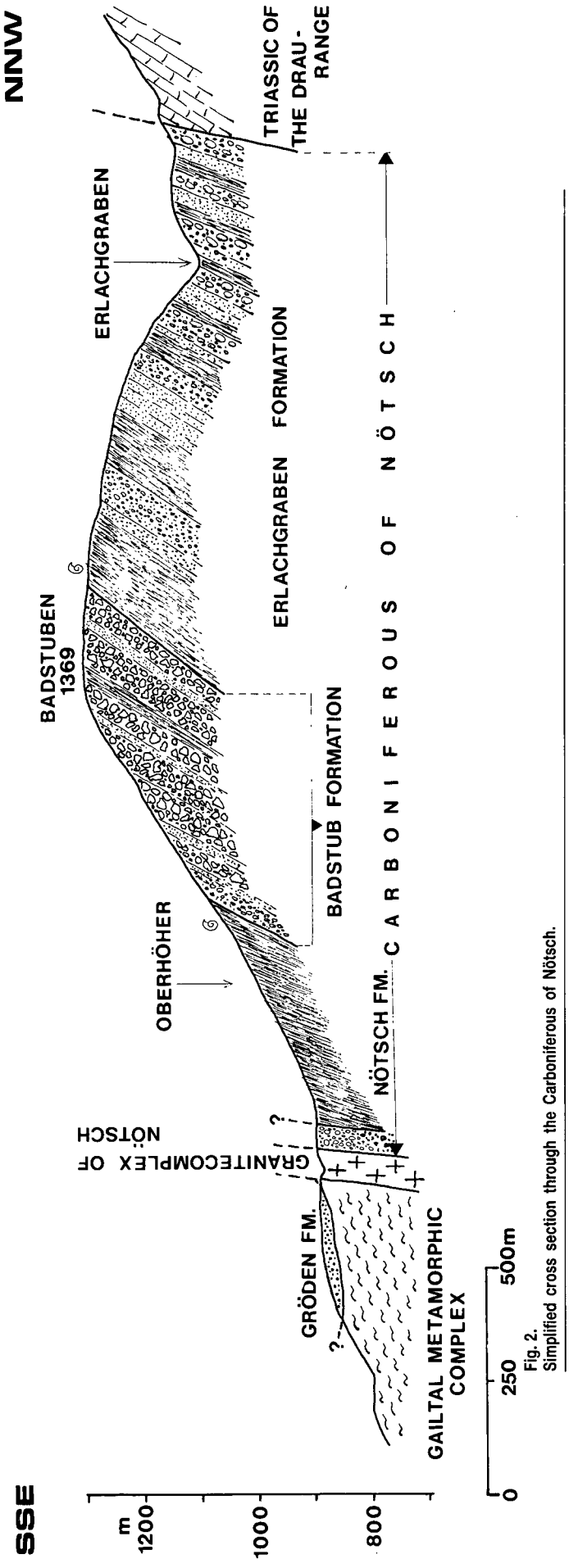

Fig. 2.
Simplified cross section through the Carboniferous of Nötsch.

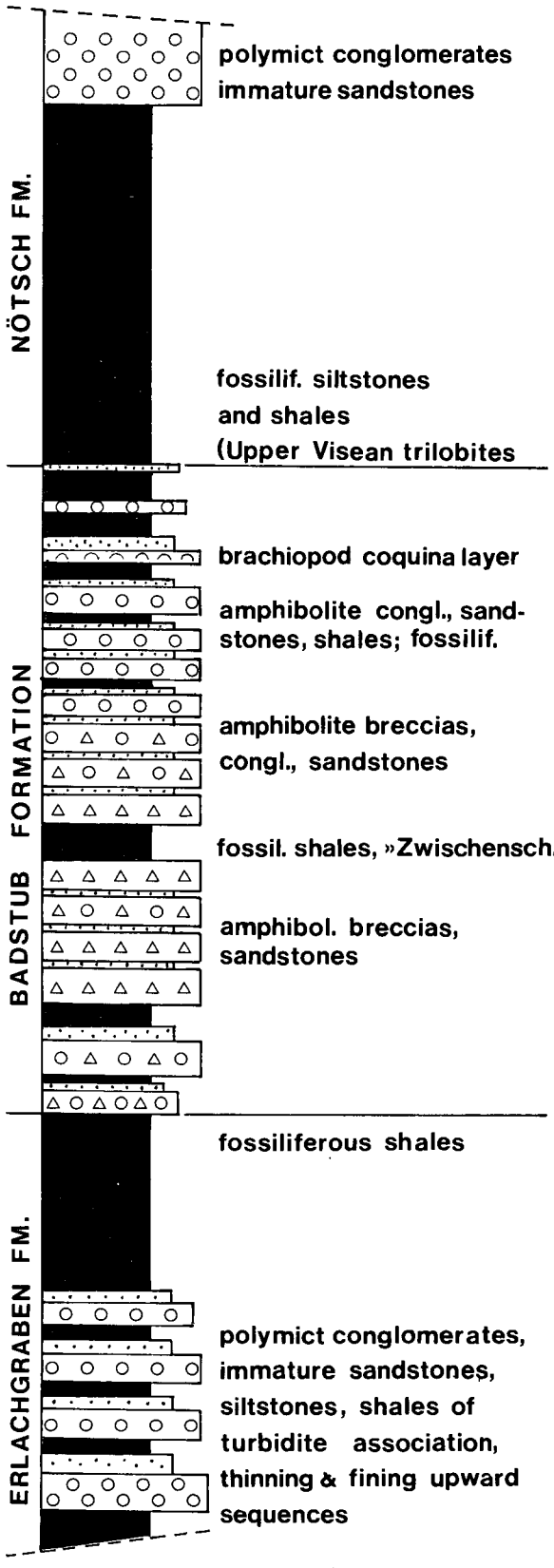

Fig. 3.
Simplified stratigraphic section of the Carboniferous of Nötsch.

3.2. Amphiboles

Chemical compositions of amphiboles

a) from coarse clastics of the Badstub Formation,
b) amphibolite clasts in the breccias and conglomerates and

Table 1a.
Representative electron microprobe analyses of amphiboles.
11,12,13 = amphibolite clasts, Badstub Formation; 14,15,16 = amphibolite (GCN); 17,18,19 = amphibolite breccia, Badstub Formation).

	11	12	13	14	15	16	17	18	19
SiO2	46,16	45,69	44,25	43,13	40,35	43,37	44,19	42,15	45,86
TiO2	0,38	0,51	0,52	0,62	0,52	0,39	0,47	0,46	0,43
Al2O3	8,61	10,33	10,10	14,89	14,13	11,60	11,07	11,40	8,53
Cr2O3	0,00	0,18	0,03	0,00	0,08	0,04	0,00	0,00	0,00
FeO	16,80	14,11	17,14	13,39	17,16	15,63	18,33	19,83	18,75
MnO	0,32	0,31	0,38	0,23	0,27	0,35	0,35	0,30	0,27
MgO	11,40	12,00	10,55	12,86	11,51	11,92	10,69	9,78	11,28
CaO	12,15	11,89	12,00	12,18	9,86	11,30	12,05	11,35	11,33
K2O	0,13	0,17	0,16	0,52	0,92	0,67	0,11	0,13	0,34
Na2O	1,24	1,70	1,48	1,61	0,91	0,81	1,12	1,68	0,88
Total	97,19	96,89	96,61	99,43	96,16	96,08	98,38	97,08	97,67
oxygens	23	23	23	23	23	23	23	23	23
Si	6,82	6,73	6,62	6,12	5,88	6,36	6,44	6,27	6,70
Ti	0,04	0,05	0,06	0,07	0,06	0,04	0,05	0,05	0,05
Aliv	1,18	1,27	1,38	1,88	2,13	1,64	1,56	1,73	1,30
Alvi	0,32	0,53	0,40	0,61	0,29	0,37	0,34	0,27	0,17
Fe3+	0,55	0,32	0,54	0,90	2,14	1,28	1,00	1,22	1,17
Fe2+	1,53	1,42	1,61	0,69	0,00	0,64	1,23	1,25	1,12
Mn	0,04	0,04	0,05	0,03	0,04	0,04	0,04	0,04	0,03
Mg	2,51	2,64	2,36	2,72	2,50	2,61	2,32	2,17	2,46
Ca	1,93	1,88	1,92	1,85	1,54	1,78	1,88	1,81	1,77
K	0,03	0,04	0,03	0,09	0,17	0,12	0,02	0,03	0,06
Na	0,36	0,49	0,43	0,44	0,25	0,23	0,32	0,48	0,25
Total	15,31	15,41	15,40	15,40	15,00	15,11	15,20	15,32	15,08

c) amphibolites from the surrounding Granite Complex of Nötsch (GCN)

have been obtained. Representative analyses and structural formulae calculated on the basis of 23 oxygens are listed in Table 1a.

The amphibole formula is calculated according to MOGESSIE et al (1989) following the recommendation of ROCK & LEAKE (1984). According to the IMA amphibole nomenclature of LEAKE (1978), the analysed amphiboles range from actinolitic hornblende to tschermakite.

The amphiboles from the three different sources (a, b and c) plot in different regions. The detrital amphiboles of the breccia always plot in a region between amphiboles of a) and c). This has been observed in Al^{IV} vs. Na + K plot (Fig. 4a).

On the diagram of LAIRD & ALBEE (1981) (Fig.4b), the amphiboles from a,b & c plot below the 1:1 line imply-

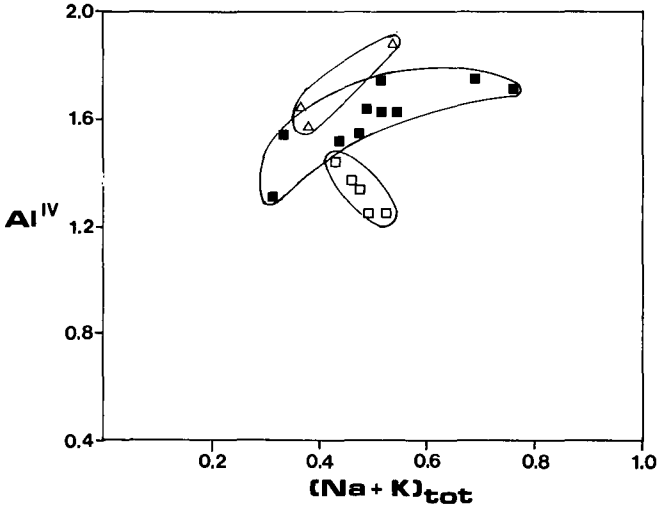

▲ a

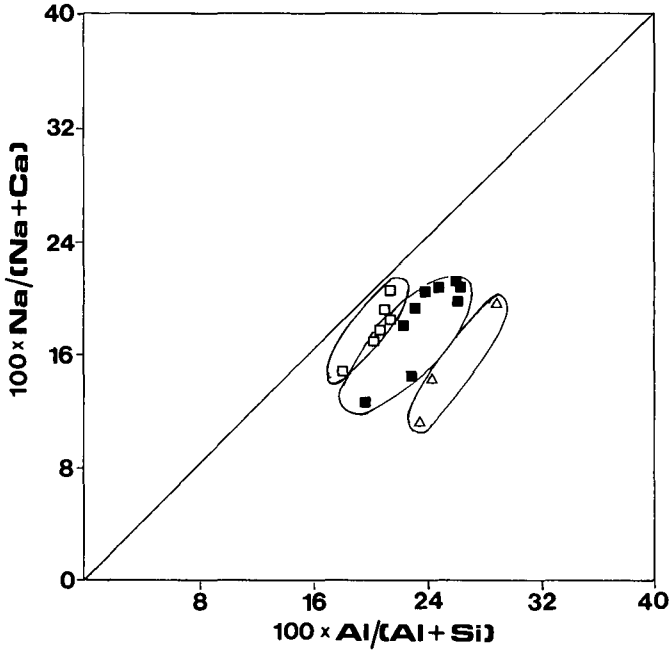

b ▶

Fig. 4.
a) Al^{IV} vs. $(Na + K)_{tot}$ plot of amphiboles.
△ = amphiboles from amphibolites of the GCN; □ = amphiboles from amphibolite clasts of the Badstub Formation; ■ = detrital amphiboles from the Badstub Formation.
b) Na/(Na + Ca) vs. Al/(Al + Si) plot of amphiboles (symbols as in Fig. 4a).

ing low to medium pressure metamorphism. In both diagrams, the amphiboles from the different sources occupy different regions which may be attributed to differences in bulk chemistry.

3.3. Feldspars

Representative electron microprobe analyses of feldspars are given in Tab. 1b and are plotted in Fig. 5. From this data, three different groups of feldspars can be distinguished (An>15, An<15 and alkalifeldspar-group with Or>9). A difference in the feldspar composition from the three different sources is not observed.

3.4. Chlorite

Representative electron microprobe analyses of chlorites are given in Tab. 1b. According to the nomenclature of HEY (1954) the chlorites range in chemistry from pycnochlorite to brunsvigite. The analysed chlorites are secondary products of hornblende.

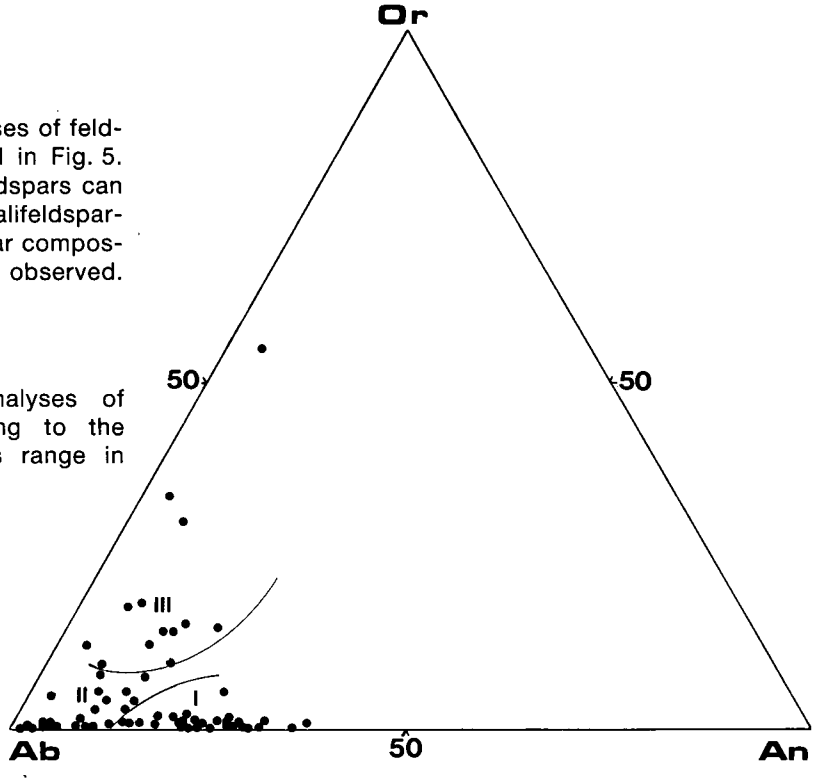

Fig. 5.
Feldspar analyses (detrital feldspars of source a, b, c) in the Or-Ab-An ternary diagram.
I = An>15 %; II = An<15 %; III = Or>9 %.

Table 1b.
Representative electron microprobe analyses of feldspars.
1,2 = detrital feldspars, Badstub Formation; 3,4 = amphibolite (GCN); 5,6 = amphibolite clasts, Badstub Formation); 7,8 = chlorite; 9,10 = epidote.

	1	2	3	4	5	6	7	8	9	10
SiO2	68,39	62,81	58,24	59,01	61,54	62,24	28,13	26,00	39,89	37,65
TiO2	0,00	0,00	0,00	0,00	0,04	0,00	0,08	0,16	0,17	0,11
Al2O3	19,79	23,07	28,76	24,86	22,38	22,82	16,15	13,07	25,97	27,72
Cr2O3	0,00	0,00	0,02	0,00	0,05	0,00	0,12	0,08	0,08	0,00
FeO	0,91	0,29	0,33	0,15	0,10	0,25	24,71	31,65	6,54	9,77
MnO	0,00	0,00	0,04	0,00	0,04	0,03	0,43	0,29	0,16	0,19
MgO	0,60	0,02	0,35	0,16	0,03	0,00	18,22	14,81	0,21	0,08
CaO	1,75	5,00	1,05	7,00	5,55	4,99	0,52	0,89	22,09	23,89
K2O	0,18	0,08	4,40	0,40	0,07	0,07	0,00	0,31	0,00	0,00
Na2O	9,34	9,50	6,48	7,42	8,75	9,52	0,08	0,11	0,00	0,00
Total	100,96	100,77	99,66	99,00	98,54	99,92	88,44	87,38	95,10	95,41
oxygens	8	8	8	8	8	8	28	28	12,5	12,5
Si	2,97	2,77	2,61	2,66	2,78	2,77	5,88	5,80	3,20	3,05
Ti	0,00	0,00	0,00	0,00	0,01	0,00	0,13	0,03	0,01	0,01
Al iv	1,01	1,20	1,52	1,32	1,19	1,20	2,10	2,17	0,00	0,00
Al vi	-	-	-	-	-	-	1,88	1,27	2,46	2,26
Fe3+	-	-	-	-	-	-	0,00	0,00	0,39	0,59
Fe2+	0,03	0,01	0,01	0,05	0,03	0,09	4,32	5,91	0,00	0,00
Mn	0,00	0,00	0,00	0,00	0,01	0,01	0,08	0,05	0,01	0,01
Mg	0,04	0,00	0,02	0,01	0,02	0,00	5,68	4,92	0,03	0,01
Ca	0,08	0,24	0,05	0,34	0,27	0,24	0,12	0,21	1,90	2,07
K	0,01	0,01	0,25	0,02	0,01	0,04	0,00	0,09	0,00	0,00
Na	0,79	0,81	0,56	0,65	0,77	0,82	0,32	0,05	0,00	0,00
Total	4,93	5,04	5,02	5,05	5,09	5,17	20,51	20,50	7,97	8,00
PS.%									13,65	20,70
Or	1,14	0,43	29,08	2,28	0,39	0,37				
Ab	89,59	77,14	65,09	64,23	73,76	77,25				
An	9,28	22,44	5,83	33,49	25,85	22,38				

3.5. Epidotes

Representative analyses of epidotes are listed in Tab. 1b. The pistacite component (stoichiometric pistacite) $Ca_3(Al,Fe^{3+})Al_2SiO_3O_{12}(OH)$ with the principal variation occurring in $Fe^{3+}(Fe^{3+} + Al)$ ranges between 13.65 % in detrital epidote grains from clastic sediments of the Badstub Formation and 20.7 % in the amphibolite clasts.

4. Bulk Chemistry

4.1. Analytical Methods

Since the amphibolite breccias and conglomerates of the Badstub Formation consist of different types of clasts, an attempt has been made to sample representative amphibolite clasts of the Badstub Formation in the field.

Major elements were determined by analysing fused samples of the amphibolite clasts of the Badstub Formation, of amphibolites of the GCN and of amphibolite breccias of the Badstub Formation with the electron microprobe according to the method described by HOINKES (1978). The trace elements Co, Cr, Cu, Li, Ni, Pb, Zn were analysed by a Philips SP9 atomic absorption spectrophotometer. Sample decomposition was made by HF-HCl-HNO_3 acid attack in Teflon bombs (PRICE 1979). The international rock standards PCC-1, W-1, G-2, AGV-1, BCR-1, BR and MRG-1 were used for calibration. Rb, Sr, Y and Zr were determined by a Philips PW X-ray fluorescence spectrometer, using linear calibration curves (corrected for Sr-Kβ interference) obtained by different US Geological Survey basaltic standards.

4.2. Major and Minor Element Chemistry

The major and minor element data of single amphibolite clasts, the breccias and conglomerates of the Badstub Formation and the amphibolites of the GCN are listed in Table 2a,b.

Table 2a.
Major and trace element analyses of amphibolite clasts of the Badstub Formation.

	AG-1	AG-2	AG-3	AG-4	AG-5	AG-6	AG-7	AG-8	AG-9	AG-10	AG-11
SiO2	49,15	46,77	46,28	45,76	45,16	46,22	44,33	46,99	45,99	44,27	46,51
TiO2	0,82	1,88	0,70	1,75	1,60	1,22	1,74	1,38	1,05	2,05	1,13
Al2O3	14,76	14,72	14,54	14,82	15,40	15,41	14,36	15,04	15,25	15,63	16,06
FeO	12,42	12,38	13,47	13,05	12,73	12,89	13,85	10,20	10,33	11,77	11,93
MnO	0,22	0,23	0,23	0,33	0,23	0,33	0,20	0,18	0,21	0,18	0,24
MgO	7,85	7,21	8,85	7,57	7,29	8,43	8,05	7,98	9,33	7,71	7,93
CaO	8,97	12,72	10,84	12,79	12,42	10,16	10,45	13,80	12,11	10,98	10,90
K2O	0,34	0,27	0,26	0,33	0,21	0,46	0,62	0,24	0,49	0,47	0,61
Na2O	4,22	2,28	3,43	2,38	2,62	3,30	2,81	2,50	3,04	4,13	3,15
P2O5	0,06	0,13	0,14	0,16	0,10	0,09	0,41	0,18	0,12	8,26	0,18
L.O.I.	1,21	1,44	1,28	1,08	2,30	1,51	3,28	1,52	2,16	2,69	1,40
Total	100,02	100,03	100,02	100,02	100,06	100,02	100,10	100,01	100,08	100,14	100,04
Zr	3	70	0	146	0	31	34	86	0	134	75
Y	0	0	50	25	16	32	0	4	0	30	16
Sr	97	266	138	131	198	228	163	130	104	142	110
Rb	0	29	3	0	0	7	0	0	107	0	0
Zn	98	86	159	91	86	83	107	52	84	83	80
Cu	41	22	10	10	61	69	54	12	20	20	32
Ni	61	72	62	87	50	73	69	76	106	85	94
Cr	21	117	30	115	21	108	71	88	254	168	133
Co	19	30	27	25	29	20	23	16	32	24	30
Li	8	62	8	15	6	16	16	6	6	8	5
Pb	16	< 10	< 10	< 10	< 10	12	12	17	23	< 10	< 10

	AG-12	AG-13	AG-14	AG-15	AG-16	AG-17	AG-18	AG-19
SiO2	47,16	47,61	51,22	46,96	49,51	51,20	47,41	49,55
TiO2	1,82	1,84	1,17	2,08	0,71	1,08	1,20	0,73
Al2O3	14,12	14,25	15,42	14,63	13,95	16,42	14,99	15,69
FeO	14,35	13,27	5,11	12,07	12,37	2,31	12,87	10,32
MnO	0,20	0,25	0,37	0,24	0,19	0,26	0,21	0,14
MgO	6,85	7,07	8,89	7,06	8,08	7,81	7,14	7,70
CaO	11,00	10,67	12,16	10,70	9,20	14,83	12,08	11,33
K2O	0,37	0,30	0,38	0,45	0,21	0,49	0,29	0,29
Na2O	2,49	2,59	3,60	3,16	4,39	2,69	2,65	2,70
P2O5	0,20	0,22	0,05	0,25	0,05	0,26	0,07	0,07
L.O.I.	1,53	1,98	1,66	2,49	1,37	2,78	1,43	1,56
Total	100,09	100,05	100,03	100,09	100,03	100,13	100,04	100,08
Zr	79	254	106	256	55	20	43	0
Y	26	0	6	8	28	25	38	15
Sr	71	56	82	105	99	119	127	454
Rb	0	0	0	29	36	0	0	5
Zn	98	97	107	84	95	54	72	59
Cu	43	45	16	22	36	15	15	58
Ni	68	72	72	105	105	78	66	84
Cr	116	109	89	111	15	195	27	262
Co	24	13	14	26	25	20	29	25
Li	8	6	4	7	5	4	4	8
Pb	<10	<10	<10	<10	<10	<10	<10	<10

Table 2b.
Major and trace element analyses of amphibolites of GCN (amph1–amph 5) and amphibolite breccias and conglomerates of the Badstub Formation (B1–B21).

	Amph 1	Amph 2	Amph 3	Amph 4	Amph 5	B-1	B-7	B-10	B-11	B-16	B-21
SiO2	52,86	59,03	52,52	50,70	61,00	44,39	52,58	45,07	52,03	53,32	52,46
TiO2	0,90	0,74	1,17	1,74	0,73	1,05	1,04	1,21	1,33	1,02	1,00
Al2O3	16,60	15,65	15,36	16,04	15,57	13,05	13,89	14,06	14,37	15,38	15,20
FeO	8,14	6,69	9,04	8,41	6,27	10,27	9,18	10,72	10,22	9,78	11,28
MnO	0,09	0,10	0,22	0,16	0,21	0,30	0,11	0,26	0,23	0,21	0,18
MgO	7,05	5,01	7,06	6,31	3,78	5,49	4,82	5,89	6,21	5,94	6, 18
CaO	8,23	5,42	8,80	9,21	5,73	14,63	9,57	12,89	8,37	7,00	7,26
K2O	0,91	0,90	1,21	0,99	0,83	0,44	0,45	0,32	0,43	0,53	0,36
Na2O	3,30	3,84	3,16	2,97	4,41	2,80	3,66	3,12	3,66	4,01	3,46
P2O5	0,19	0,14	0,23	0,27	0,12	0,12	0,09	0,19	0,21	0,10	0,11
L.O.I.	1,78	2,77	1,32	3,40	1,42	8,10	4,46	6,73	3,03	2,79	2,61
Total	100,05	100,29	100,09	100,20	100,07	100,64	99,85	100,46	100,09	100,08	100,10
Zr	104	183	118	270	166	16	79	122	180	53	124
Y	0	52	31	6	0	12	77	49	47	27	19
Sr	209	180	143	32	209	196	147	176	193	227	206
Rb	24	23	50	6	0	75	0	20	0	17	0
Zn	58	60	86	66	43	79	77	89	65	49	65
Cu	78	38	45	30	22	177	98	127	80	58	51
Ni	115	64	90	73	<10	52	49	59	65	54	54
Cr	171	77	191	139	<10	74	61	64	97	93	83
Co	5	24	19	18	<5	13	11	15	11	8	11
Li	9	17	6	23	6	13	6	6	9	20	10
Pb	<10	<10	<10	<10	<10	16	<10	<10	<10	<10	<10

From their textural features and mineralogical assemblages, the amphibolites are considered to be of magmatic origin. In order to determine the magma type of the amphibolite clasts and the amphibolites in the GCN the analyses are plotted on different discrimination diagrams available in the literature.

According to MIYASHIRO (1973) the FeO_{tot}, MgO, SiO_2 and TiO_2 contents usually suffer relatively little change during metamorphism and other secondary processes.

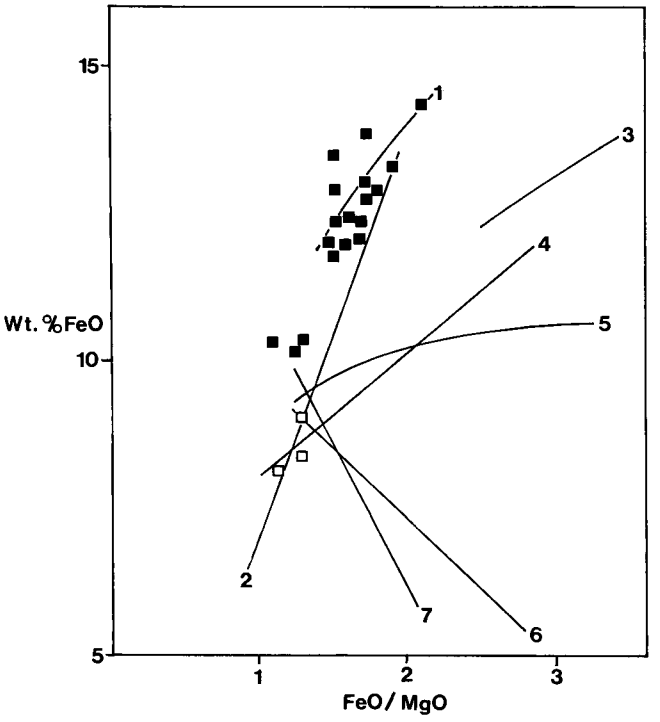

Fig. 6.
FeO vs. FeO/MgO plot (after MIYASHIRO 1973).
FeO = FeO_{tot}.
1 = Skaergaard-tholeiite; 2 = ocean floor basalts; 3–7 = different island arc basalts.
■ = amphibolite clasts of the Badstub Formation; □ = amphibolites of the GCN.

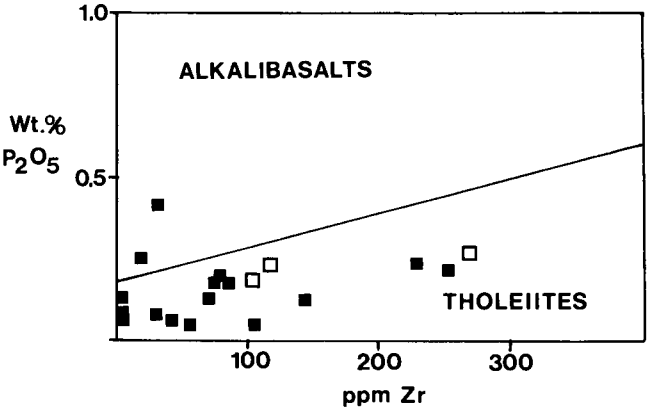

Fig. 7.
P_2O_5 vs. Zr plot (after WINCHESTER & FLOYD 1976).
Symbols as in Fig. 6.

He suggested that relations such as FeO_{tot} vs. FeO_{tot}/MgO and TiO_2 vs. FeO_{tot}/MgO are particularly useful in the study of rocks of older geological ages. A plot of the chemical data on the FeO_{tot} vs. FeO_{tot}/MgO diagram (Fig. 6) indicates a similar trend to the Skaergaard tholeiitic magma and the abyssal tholeiites of Greenland.

Several authors (PEARCE & CANN, 1971, 1973; WINCHESTER & FLOYD, 1976,1977; FLOYD & WINCHESTER, 1978) suggested the use of immobile elements to characterize altered and metamorphosed magmatic rocks in terms of magma series (alkaline, subalkaline) and degree of differentiation (basaltic, andesitic etc.).

Plot of P_2O_5 vs. Zr (Fig. 7) shows a tholeiitic magma trend for most of the amphibolite clasts, only two samples have alkaline affinity. The tholeiitic nature of the magma can also be seen in Fig. 8, where almost all the samples plot in the tholeiitic region. However, the amphibolites from the GCN occupy a field denoted by higher MgO and Na_2O + K_2O compared to the amphibolite clasts.

According to PEARCE et al. (1975) the TiO_2-K_2O-P_2O_5 diagram (Fig. 9) helps to differentiate continental basalts from oceanic basalts. The chemical data of the

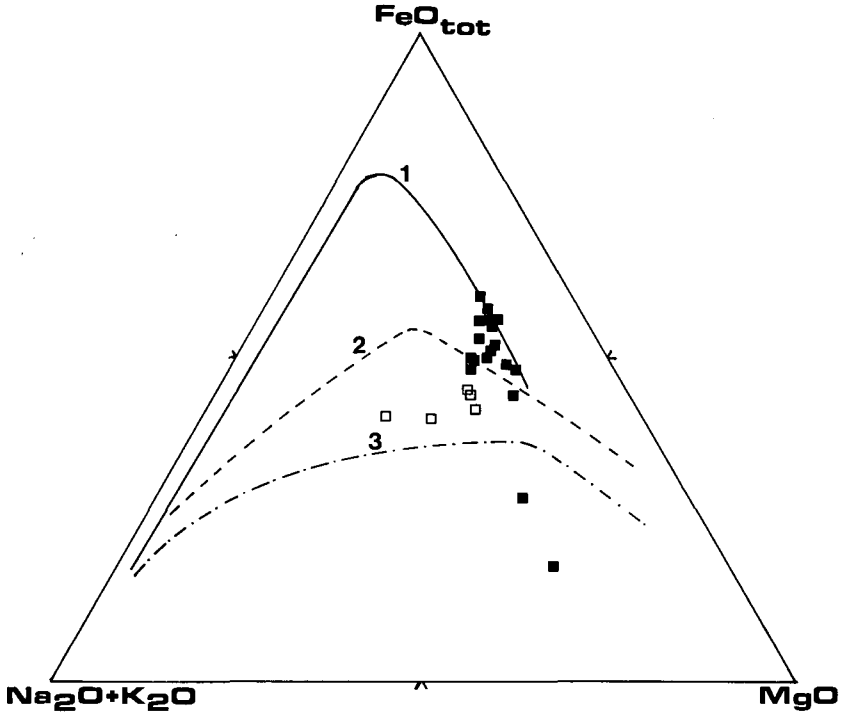

Fig. 8.
FeO_{tot} – Na_2O + K_2O – MgO plot.
1 = Trend of tholeiitic Skaergaard-melts (WAGNER, 1960); 2 = alkali-trend (MACDONALD & KATSURA, 1964); 3 = calcalkali-trend (TURNER & VERHOOGEN, 1960).
Symbols as in Fig. 6.

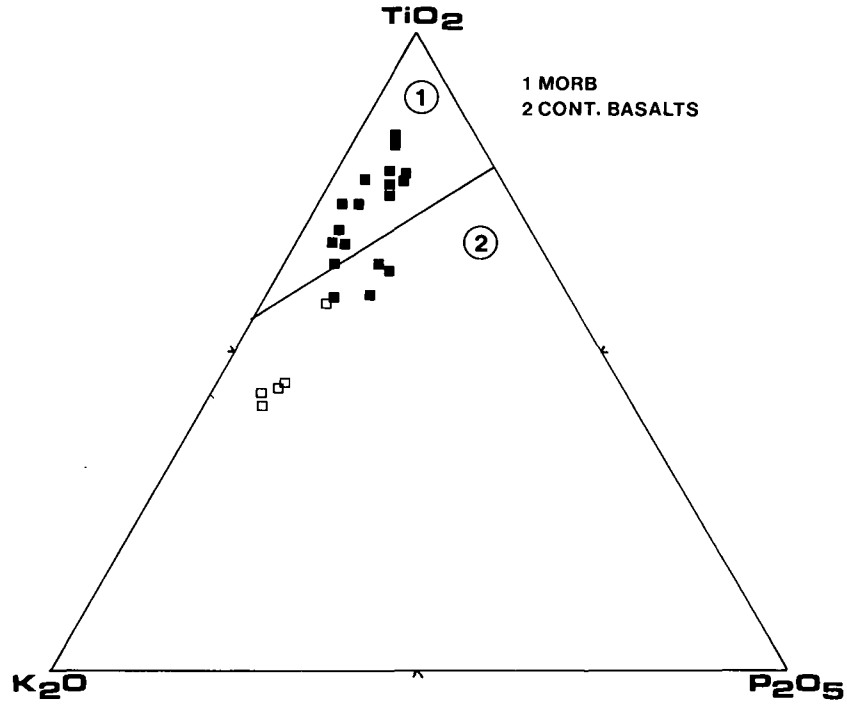

Fig. 9.
TiO_2 – K_2O – P_2O_5 plot.
After PEARCE et al. (1975).
Symbols as in Fig. 6.

amphibolite clasts and amphibolites of the GCN are plotted on this diagram. Most of the analyses of the amphibolite clasts plot in the mid ocean-ridge basalt field. Some amphibolite clasts (which could have been altered) and the amphibolites of the GCN plot in the continental basalt region.

A plot of Ti/Cr vs. Ni in Fig. 10 shows that most of the amphibolite clasts and the amphibolites of the GCN occupy a region within the ocean floor basalts. The two amphibolite clast samples which plot in the island arc basalt field are those which are considered to be altered in Fig. 9.

5. Lithofacies

5.1. Structural and Textural Features of the Badstub Formation

The Badstub Formation (approximately 400 m thick), overlying thick fossiliferous shales, is a sequence of mainly amphibolite-rich breccias and conglomerates with intercalated sand-siltstones and silty shales which contain fossils at some places.

In the lower part of the Badstub Formation fine-grained, silty-sandy sediments dominate with some up

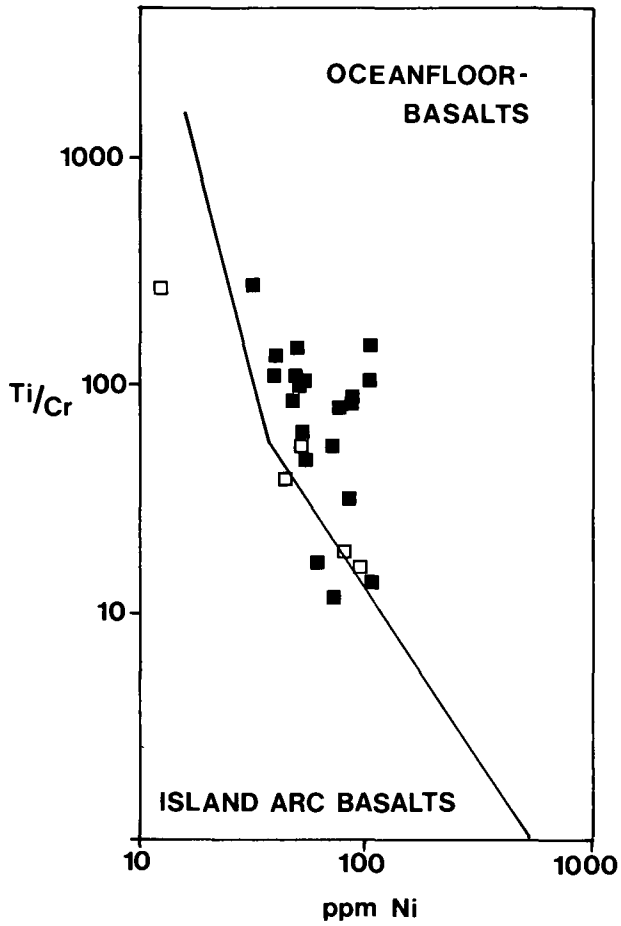

Fig. 10.
Ti/Cr vs. Ni plot.
After BECCALUVA et al. (1979).
Symbols as in Fig. 6.

to about 2 meters thick intercalated amphibolite-breccias (Fig. 12). In the middle part of the sequence which is most completely exposed in the "Jakomini Quarry" of the Nötschgraben, amphibolite-breccias with thicknesses of the single beds measuring up to about 2 meters dominate. Intercalated are dm thick sandstones and siltstones. Approximately in the middle of the sequence a several m thick shale ("Zwischenschiefer") containing a rich fauna (esp. brachiopods and corals) is intercalated.

In the upper part of the Badstub Formation, the clasts are better rounded. The sequence is built up by interstratified conglomerates rich in amphibolite-clasts, sandstones and siltstones frequently forming small scale fining upward cycles grading into fossiliferous siltstones and shales with a few conglomerate- and sandstone layers (Fig. 11). Within this upper part a several dm thick coquina-layer, composed of brachiopod-shells and spines, a few corals and foraminiferes, embedded in a dark, shaly-silty groundmass, has been recognized (Fig. 11,13).

The middle and upper parts of the Badstub Formation may be compared with the turbidite facies A (arenaceous-conglomeratic facies) of MUTTI & RICCI LUCCHI (1978).

The sheet-like breccia beds with thicknesses ranging up to about 2 meters frequently show crudely to well developed normal graded bedding ("graded beds" of WALKER, 1975, 1977, „normally graded gravel" of PICKERING et al. 1989; Fig. 14). Within a few beds crudely

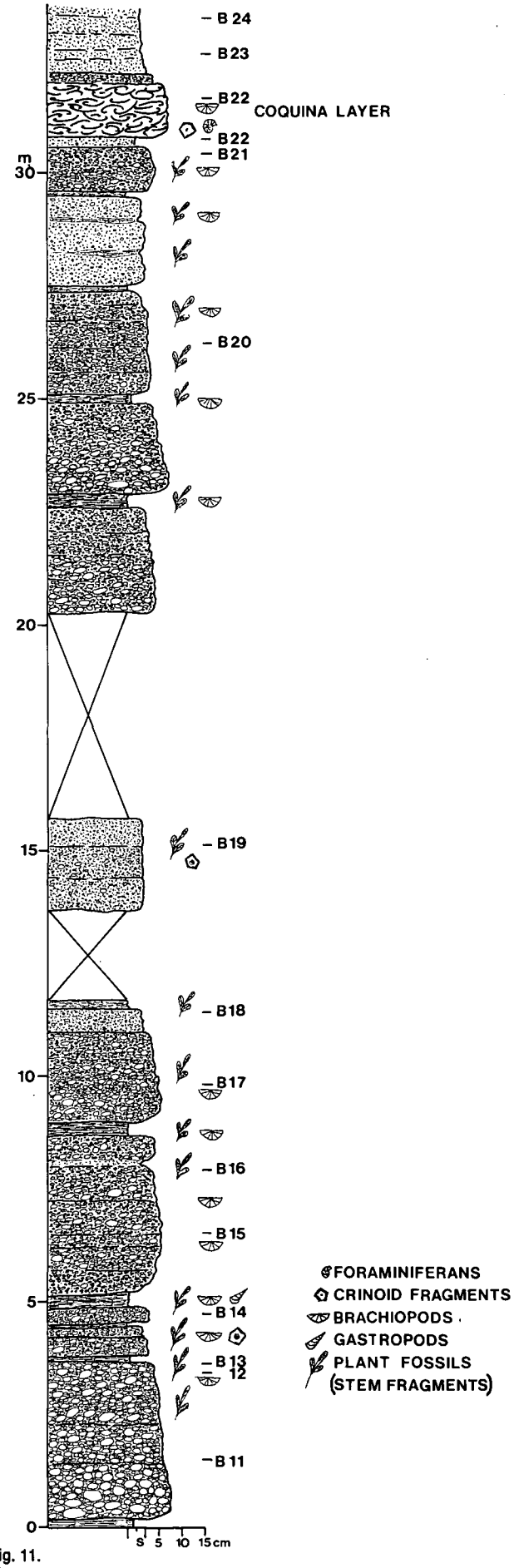

Fig. 11.
Measured vertical profile through the upper (conglomeratic) part of the Badstub Formation.

Fig. 12.
Poorly sorted, clast-supported amphibolite breccia composed of different types of angular amphibolite clasts and a few carbonate clasts.

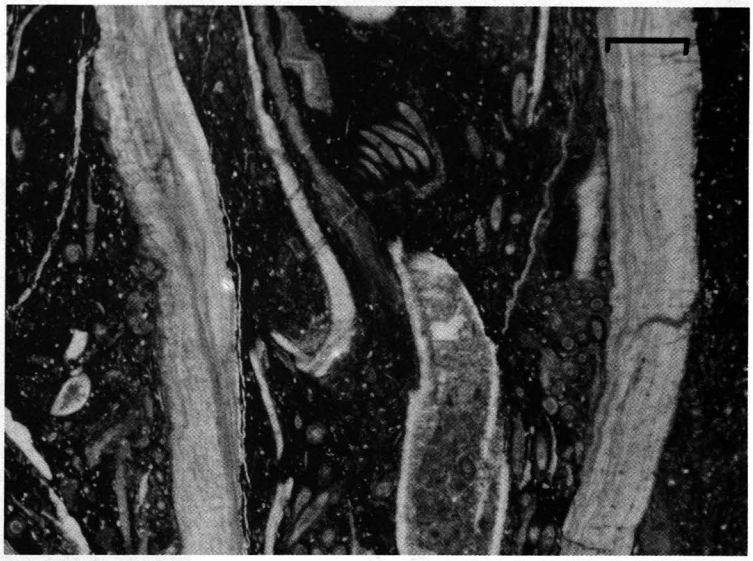

Fig. 13.
Photomicrograph of the coquina layer with brachiopod shells and spines and a foraminifer (*Tetrataxis*), embedded in a dark, shaly groundmass.
Scale bar is 1 mm.

Fig. 14.
Fine-grained amphibolite breccia with well developed normal graded bedding and crudely developed inverse grading at the base.
At the top coarse- and fine-grained sandstone.

developed inverse grading at the base has been observed, corresponding to the "inverse- to- normally graded model" of WALKER (1975, 1977). Sorting is very poor and the clasts in most cases form a clast-supported framework (Fig. 12,16). In some beds a chaotic, matrix-supported framework ("disorganized beds" after WALKER, 1975, 1977; "disorganized gravel" of PICKERING et al., 1989) is observed (Fig. 17).

Most clasts are angular and a few are better rounded (subangular to subrounded). The maximum clast

Fig. 15.
Photomicrograph of a laminated, graded, immature sandstone rich in amphibolite fragments and detrital amphiboles.
Scale bar is 1 mm.

diameter seldom exceeds 35 cm, in most cases is below 20 cm. The clasts are embedded in a sandy matrix.

In the upper part conglomerates with better rounded clasts (subangular to subrounded) and maximum diameters below 10 cm dominate. Breccias and conglomerates displaying graded bedding frequently are overlain by sandstones with thicknesses up to a few dm (Bouma divisions A, B). The sandstones frequently show horizontal lamination and normal graded bedding ("parallel stratified sand" after PICKERING et al., 1989; Fig. 15). In the lower and upper parts of the Badstub Formation sandstones sometimes grade into laminated or massive siltstones ("structureless silt" and "graded stratified silt" after PICKERING et al., 1989) and silty shales probably representing Bouma divisions D and E(t).

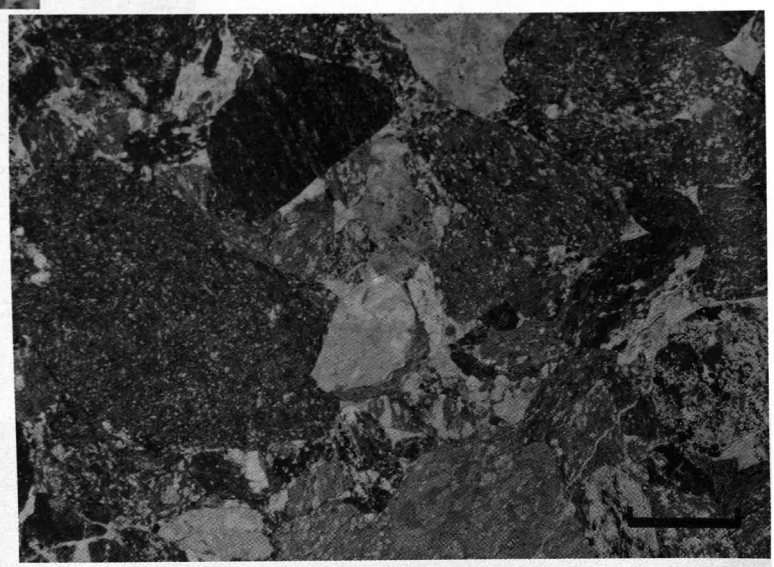

Fig. 16.
Photomicrograph of a clast-supported, fine-grained amphibolite conglomerate with different types of amphibolite clasts.
Scale bar is 2 mm.

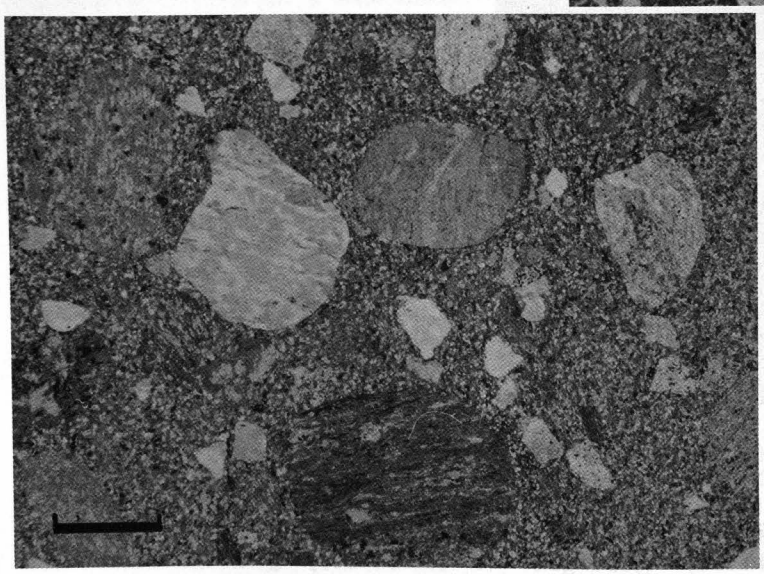

Fig. 17.
Photomicrograph of a matrix-supported, fine-grained conglomerate. Rounded amphibolite clasts and a few metamorphic clasts are embedded in a sandy groundmass rich in detrital amphiboles.
Scale bar is 2 mm.

5.2. Composition of the Sediments of the Badstub Formation

The most frequent clasts in the breccias and conglomerates are different types of amphibolites. In the coarse-grained varieties up to about 80 % of the clasts are of this type. In the fine-grained breccias and conglomerates the content of amphibolite clasts ranges between 60 % in the middle part to 40 % in the upper part of the sequence (average values, see Table 3, Fig. 16).

Table 3.
Average composition of breccias and conglomerates of the Badstub Formation.

		Amph-cl	o. MRF	Qp	Carb-cl	M
Middle part	(12)	61	16	2	2	19
Upper part	(14)	42	28	5	1	24
	(6)	46	25	2	2	25

Amph-cl = amphibolite clasts; o. MRF = other metamorphic rock fragments; Qp = polycrystalline quartz; Carb-cl = carbonate clasts; M = matrix.

The other clasts are gneisses, schists, quartzites and carbonates (marbles, rarely grey limestones containing conodonts SCHÖNLAUB, 1985). The matrix content ranges from 4l in densly packed conglomerates and breccias to about 50 % in matrix-supported breccias and conglomerates (Fig. 17).

The sandy matrix is composed of poorly sorted, angular amphiboles (hornblende), amphibolite fragments, different metamorphic rock fragments mostly derived from gneisses and schists, detrital feldspars (plagioclases), detrital epidote, mono- and polycrystalline quartz, a few detrital garnets, phyllosilicate-cement and calcite cement.

Sandstones are texturally and compositionally immature (very poorly to poorly sorted, angular to subangular), showing nearly the same composition as the sandy matrix of the breccias and conglomerates (see Table 4).

5.3. Fossil Content and Age of the Badstub Formation

Fossils (without stratigraphic significance) are found in the several m thick shale member in the middle part of the sequence ("Zwischenschiefer", brachiopods, corals and other), in conglomerates (brachiopods, crinoid stem fragments and plant fossils, see Fig. 18), sandstones (brachiopod shells and spines, crinoid stem fragments, foraminifers and plant fossils), shales (brachiopods, bivalves, crinoid stem fragments and plant fossils) and the coquina layer in the upper part of the sequence (Fig. 13).

Upper Visean conodonts obtained from grey limestone clasts of the Badstub Formation by SCHÖNLAUB (1985) and an Upper Visean trilobite fauna from shales overlying the Badstub Formation (HAHN & HAHN, 1987) indicate that this breccia was deposited within a very short period during the Upper Visean.

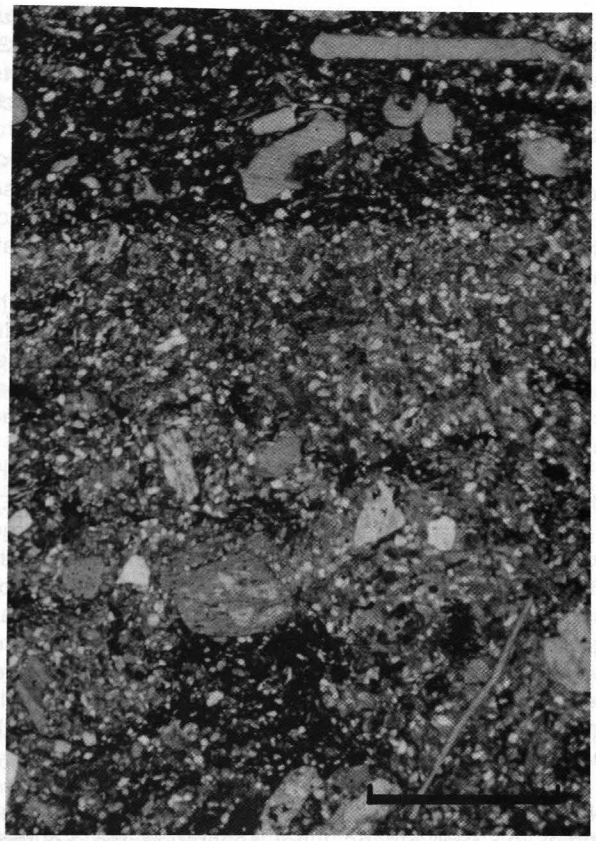

Fig. 18.
Photomicrograph of an immature, coarse-grained sandstone rich in amphibolite fragments and detrital amphiboles, containing a few fossil fragments (echinoderm fragments and others).
Scale bar is 2 mm.

6. Origin of the Badstub Formation

6.1. Source Region of the Amphibolite Clasts

As discussed in the foregoing paragraph, the amphibolites are assumed to be of magmatic origin, and different variation diagrams have proved that the magma type is tholeiitic (Figs. 6,7,8,10). These amphibolite clasts were probably metamorphosed during the Hercynian time. Their mineral assemblages and mineral compositions (Table 2a,b) indicate an amphibolite facies metamorphic grade. Textural features and fossils of the Badstub Formation clearly indicate a sedimentary origin of the breccias, conglomerates and associated sediments rich in resedimented amphibolite clasts and amphibolite-derived material.

Table 4.
Average composition of sandstones of the Badstub Formation.

	Qm	Qp	Fsp	Hb	Ep	Am	MRF	Cc	M
Middle part (5)	3	4	11	33	5	15	11	5	13
Upper part (3)	5	8	15	19	7	5	22	2	17

Qm = monocrystalline quartz; Qp = polycrystalline quartz; Fsp = detrital feldspar; Hb = detrital hornblende; Ep = detrital epidote; Am = amphibolite fragments; MRF = metamorphic rock fragments; Cc = calcite cement; M = matrix.

The metamorphic and tholeiitic nature of the Badstub Formation has also been documented by TEICH (1982), although he did not sample single amphibolite clasts, but presented chemical analyses of the whole breccia which is made up of different components.

The significant problem is to determine the source region of these amphibolite clasts. For this purpose, comparative geochemical and stratigraphic work on the amphibolites of GCN and these amphibolite clasts has been undertaken.

The amphibolites of GCN which are found in the southern part of the Carboniferous of Nötsch have different geochemical patterns and plot in different fields of the variation diagrams employed. Therefore one cannot consider a similar origin for the amphibolite clasts and the amphibolites of GCN.

A comparison of the amphibolite clast data and those of Veitsch metavolcanics (PROHASKA & EBNER, 1989) shows a similarity both in magma type and tectonic position. However, the amphibolite clasts of the Badstub Formation are found to be part of a mappable sedimentary sequence which could have important geological significance compared to the small lenses or bands of the Veitsch metavolcanics whose source region also is not known. Although they are of similar magma type and tectonic position it is difficult to make a correlation.

Mapping (Fig. 1) has shown that the Carboniferous of Nötsch lies in the northern part of an important tectonic line (Periadriatic Line) separating the Southern Alps from the Eastern Alps. When one considers the tectonic position of the Badstub Formation and the general Alpine mountain building process, there seems to be a dextral strike slip movement along the Periadriatic Line which placed the Badstub Formation in its present positon. Considering the tectonic position occupied by the analytical data of the amphibolite clasts on the different variation diagrams (Figs. 9,10) the original position of the amphibolite clasts is in an oceanic crustal environment.

6.2. Sedimentological Evidence of the Origin of the Badstub Formation

Following the facies model of WALKER (1975, 1977) for resedimented conglomerates of turbidite associations, the following lithofacies-types can be recognized: disorganized, graded-bed and inverse to normally graded conglomerates/breccias.

Disorganized, in most cases matrix supported breccias and conglomerates may be interpreted as cohesive debris flows (LOWE, 1979, 1982) or "true debris flows" (after MIDDLETON & HAMPTON, 1973, 1976), where the larger clasts were supported by the buoyancy and cohesiveness of the sediment-water matrix. Disorganized breccias and conglomerates may also originate from high concentration turbidity currents (PICKERING et al., 1989). According to WALKER (1975, 1977), disorganized beds are probably characteristic of submarine feeder channels or canyons. Normal graded breccia and conglomerate beds seem to be most frequent, although there are all transitions to disorganized beds.

Inverse grading at the base of some of the breccia and conglomerate beds indicate a graded traction carpet layer resulting from dispersive pressure arising from grain collisions during flow. This inverse to normally graded lithofacies is interpreted to be formed from gravelly high density currents with a basal inversely graded traction carpet layer overlain by normally graded suspension sedimentation (LOWE, 1982). Or these beds were probably combined grain flows/debris flows as discussed by HAMPTON (1979) and density-modified grain flows (LOWE, 1976), which tended to evolve forward as high density turbidity currents (LOWE, 1982; WALKER, 1975, 1977). Following the concept of WALKER (1975, 1977), the inverse to normally graded model reflects flow on a relatively steep slope and passes into the graded and the graded-stratified model as the slope flattens out on the midfan (see also WALKER, 1978, 1984).

The horizontal laminated, normally graded sandstones, frequently overlying conglomerate/breccia beds, are interpreted to be formed by sandy, high-density turbidity currents in the sense of LOWE (1982). The siltstone-layers which sometimes occur on top of the thinning- and fining-upward cycles probably originated from low-density turbidity currents, representing the "dilute tail" to the underlying high-density current sandstones (see also PICKERING et al., 1989).

Such thinning- and fining-upward cycles, which are frequently found within the Badstub Formation, esp. in its upper part, are commonly used to recognize channel deposits of submarine fans (MUTTI & RICCI LUCCHI, 1972; SHANMUGAM & MOIOLA, 1988). These sediments also form on small slope aprons along active fault zones as reported by STOW (1985) from the Upper Jurassic Brae Oilfield Turbidite System of the North Sea. Shallow-water fossils within coarse- and fine-grained sediments of the Badstub Formation indicate sedimentation in a proximal, probably relatively shallow marine environment below wave base. Similar sediments containing fossils have been described by SURLYK (1978, 1984) from the Jurassic/Cretaceous of East Greenland and interpreted as small submarine fans (continental borderland fans) formed along fault scarps. The several m thick fossiliferous dark shales ("Zwischenschiefer") probably represent interfan mudstones.

In conclusion, the Badstubbreccia Complex is believed to represent a sedimentary sequence of submarine resedemented breccias, conglomerates, sandstones and siltstones formed by sediment gravity flows on a proximal fan or slope (slope apron, fan delta) along an active fault zone. Due to the lack of exposures the lateral facies distribution and transport direction is not known. The high content of amphibolite-derived material which is highly susceptible to weathering processes, and the coarse grain-size, indicate very rapid sedimentation, caused by tectonic movements at an active fault zone.

7. Discussion

The amphibolite breccias and conglomerates of the Badstub Formation in the Carboniferous of Nötsch represent submarine proximal fan or slope (slope apron,

fan delta) deposits of Upper Visean age, formed by different types of sediment gravity flows.

The amphibolite clasts are derived from metamorphosed tholeiitic ocean floor basalts. As there is no evidence for a subduction zone and related arc-trench system (no volcanic arc derived material etc), the sediments probably formed along a fault zone of a passive margin active during Upper Visean.

The strong overprinting of the Paleozoic basement of the Alpine-Mediterranean by Alpine metamorphism and tectonics, and the fact that the Carboniferous of Nötsch is tectonically isolated as a result of lateral movements along the Periadriatic Line during the Alpine tectonic cycle makes it difficult to present a paleogeographic reconstruction and geodynamic interpretation.

In general, the Upper Devonian – Lower Carboniferous was marked by convergence of Gondwana (or parts of Gondwana) and Laurasia (ZIEGLER, 1986), accompanied by large dextral transform faults (ARTHAUD & MATTE, 1977; MATTE, 1986; ZIEGLER, 1982, 1986), which are explained by westward drifting of the African plate (Gondwana) and the Eurasian plate (Laurasia) linking the Urals and Appalachians (ZIEGLER, 1984; VAI & COCOZZA, 1986).

During this transform rifting phase from Upper Devonian to Lower Silesian (VAI & COCOZZA, 1986) several microplates outlined by zones of thinned sialic crust were generated, with narrow seaways between them.

As pointed out by VAI & COCOZZA (1986) and MATTE (1986) based on relatively few paleomagnetic data (IRVING, 1977; SMITH, 1981; VAN DER VOO, 1982) large oceans between Laurasia and Gondwana did not exist during Upper Devonian – Lower Carboniferous. Moreover the Variscan deformation is the result of the collision of small microplates ("terranes", see FRISCH & NEUBAUER, 1989) with Laurasia which detached from Gondwana (see also ZIEGLER, 1984). During this time interval a large-scale westward drifting of some microplates like the Carnic-Dinaridic microplate took place (VAI, 1976, 1979).

The Carboniferous of Nötsch, now situated immediately north of the Periadriatic Line, was originally probably linked to the deep-sea clastics of the south alpine Hochwipfel Fm. and therefore part of the Southern Alps. This idea is also supported by exotic limestone clasts from the Hochwipfel and Badstub Formation, which are of the same age and display the same microfacies types and therefore are probably derived from the same source (FLÜGEL & SCHÖNLAUB, 1990).

From the petrographic, mineralogic and sedimentologic data presented in the foregoing sections, the sediments of the Carboniferous of Nötsch, especially those of the Badstub Formation, were most likely deposited at an active fault zone (?transform fault) of a relatively narrow seaway between the Carnic-Dinaridic microplate and an East Alpine microplate, which opened during large-scale transcurrent faulting and rifting as proposed by VAI (1979) and VAI & COCOZZA (1986).

Although the exact age of metamorphism of the amphibolite clasts is not known, metamorphism of tholeiitic ocean floor basalts probably took place during an early stage of transform faulting along a fracture zone. Similar processes have recently been described from the Vema fracture zone of the equatorial Mid-Atlantic Ridge by HONNOREZ et al. (1984). It is suggested that during a later stage of transform faulting and rifting, this metamorphosed ocean floor basalts were redeposited on small submarine fans or slope aprons along an active fault zone, forming the amphibolite breccias and conglomerates of the Badstub Formation.

Acknowledgments

This research was supported by the Fonds zur Förderung der wissenschaftlichen Forschung in Österreich, Project P6651 E. We thank Prof. Dr. H. MOSTLER (Innsbruck), Prof. EBNER, Doz. PROHASKA and Dr. MCELDUFF (Leoben) for critical comments, and Dr. TESSADRI (Innsbruck) for the trace element analyses. AM would like to thank Prof. PURTSCHELLER for his permission to use the research facilities of the institute of Mineralogy and Petrography, University of Innsbruck during the progress of the project and Prof. STUMPFL (Leoben) for his encouragement and support during the preparation of the manuscript.

References

ANGEL, F. (1932): Diabase und deren Abkömmlinge in den österreichischen Ostalpen. – Mitt. naturwiss. Ver. Steiermark, **69**, 5–24, Graz.

ARTHAUD, F. & MATTE, P. (1977): Late Paleozoic strike-slip faulting in Southern Europe and North Africa: results of a right lateral shear zone between the Appalachians and the Urals. – Geol. Soc. Am. Bull., **88**, 1305–1320, Boulder.

BECCALUVA, L., OHNENSTETTER, P & OHNENSTETTER, M. (1979): Geochemical discrimination between ocean-floor and island-arc tholeiites – application to some ophiolites. – Can. J. Earth Sci., **16**, 1874–1882.

BENCE, A.E. & ALBEE, A.L. (1968): Empirical correction factors for the electron probe micro-analyses of silicates and oxides. – J. Geol., **76**, 382–403, Chicago.

FELSER, T.O. (1936): Die Badstub-Breccie der Karbonscholle von Nötsch im Gailtal (Kärnten). – Zentralbl. Mineral. Geol. Paläont. B., **8**, 305–308, Stuttgart.

FLOYD, &.A. & WINCHESTER, J.A. (1978): Identification and discrimination of altered and metamorphosed volcanic rocks using immobile elements. – Chem. Geol., **21**, 231–306, Amsterdam.

FLÜGEL, E. & SCHÖNLAUB, H.&. (1990): Exotic limestone clasts in the Carboniferous of the Carnic Alps and Nötsch. – In: VENTURINI, C. & KRAINER, K. (1990): Field Workshop on Carboniferous to Permian Sequence of the Pramollo-Nassfeld Basin (Carnic Alps). – Proceedings (pre-print), 15–19, Udine.

FRECH, F. (1894): Die Karnischen Alpen. – Halle (M. Niemeyer) 514p.

FRISCH, W. & NEUBAUER, F. (1989): Pre-Alpine terranes and tectonic zoning in the Eastern Alps. – Geol.Soc. Am., Spec. Paper, **230**, 91–100, Boulder.

HAHN, G. & HAHN, R. (1987): Trilobiten aus dem Karbon von Nötsch und aus den Karnischen Alpen Österreichs. – Jb. Geol. B.-A., **129**/3+4, 567–619, Wien.

HAMPTON, M.A. (1979): Buoyancy in debris flows. – Jour. Sed. Petrol., **49**, 753–758, Tulsa.

HEY, M.H. (1954): A new review of chlorites. – Min. Magazine, **30**, 277–292, London.

HOINKES, G. (1978): Zur Mineralchemie und Metamorphose toniger und mergeliger Zwischenlagen in Marmoren des südwestlichen Schneebergerzuges (Ötztaler Alpen, Südtirol). – N. Jb. Miner. Abh., **131**, 272–303, Stuttgart.

HONNOREZ, J., MEVEL, C. & MONTIGNY, R. (1984): Occurrence and significance of gneissic amphibolites in the Vema fracture zone, equatorial Mid-Atlantic Ridge. – In: GASS, I.G., LIPPARD, S.J. & SHELTON, A.W. (Eds.): Ophiolites and Oceanic Lithosphere, Geol. Soc. Spec. Publ., **13**, 121–130, Oxford.

IRVING, E. (1977): Drift of the major continental blocks since the Devonian. – Nature, **270**, 304–309, London.

KIESLINGER, F. (1956): Die nutzbaren Gesteine Kärntens. – Carinthia II, Sdh. **17**, 384p., Klagenfurt.

KODSI, G.M. & FLÜGEL, H.W. (1970): Lithofazies und Gliederung des Karbons von Nötsch. – Carinthia II, **160**/80, 7–17, Klagenfurt.

LAIRD, J. & ALBEE, A.L. (1981): Pressure, temperature and time indicators in mafic schist: their application to reconstructing the polymetamorphic history of Vermont. – Am. J. Sci., **281**, 127–175, New Haven, Conn.

LEAKE, B.E. (1978): Nomenclature of amphiboles. – Am. Mineralogist, **63**, 1023–1052, Richmond, Virginia.

LOWE, D.R. (1976): Subaqueous liquefied and fluidized sediment flows and their deposits. – Sedimentology, **23**, 285–308, Oxford.

LOWE, D.R. (1979): Sediment gravity flows: their classification and some problems of application to natural flows and deposits. – Soc. Econ. Paleont. Mineral., Spec. Publ., **27**, 75–82, Tulsa.

LOWE, D.R. (1982): Sediment gravity flows: II. Depositional models with special reference to the deposits of high-density turbidity currents. – Jour. Sed. Petrol., **52**, 279–297, Tulsa.

MACDONALD, G. & KATSURA, T. (1964): Chemical composition of Hawaiian lavas. – J. Petrol., **5**, 82–113, Oxford.

MATTE, P. (1986): Tectonics and plate tectonic model for the Variscan belt of Europe. – Tectonophysics, **126**, 329–374, Amsterdam.

MIDDLETON, G.V. & HAMPTON, M.A. (1973): Sediment gravity flows: mechanics of flow and deposition. – In: Turbidites and Deep-Water Sedimentation: Soc. Econ. Paleont. Mineral., Pacific Section Short Course Lecture Notes, p. 1–38, Tulsa.

MIDDLETON, G.V. & HAMPTON, M.A. (1976): Subaqueous sediment transport and deposition by sediment gravity flows. – In: STANLEY, D.J. & SWIFT, D.J.&. (Eds.): Marine Sediment Transport and Environmental Management, New York (Wiley) 197–218.

MIYASHIRO, A. (1973): The Troodos Ophiolithic Complex was probably formed in an island arc. – Earth Planet. Sci. Lett., **19**, 218–224, Amsterdam.

MOGESSIE, A., TESSADRI, R. & VELTMAN, C.B. (1990): EMP - AMPH - a Hypercard program to determine the name of an Amphibole from Electron Microprobe Analysis according to the International Mineralogical Association Scheme. – Computers and Geosciences, **16**, 309–330.

MUTTI, E. & RICCI LUCCHI, F. (1978): Turbidites of the Northern Apennines: Introduction to Facies Analysis. – Internat. Geology Rev., **20**, 125–166, Falls Church, Virginia.

PEARCE, J. (1975): Basalt geochemistry used to investigate past tectonic encironments on Cyprus. – Tectonophysics, **25**, 4–67, Amsterdam.

PEARCE, J. & CANN, J. (1971): Ophiolite origin investigated by discriminant analysis using Ti, Zr, and Y. – Earth Planet. Sci. Lett., **12**, 339–349, Amsterdam.

PEARCE, J. & CANN, J. (1973): Tectonic setting of basic volcanic rocks determined using trace element analysis. – Earth Planet. Sci. Lett., **19**, 290–300, Amsterdam.

PEARCE, T.H., GORMANN, B.E. & BIRTETT, T.C. (1975): The TiO_2–K_2O-P_2O_5 diagram: a method of discriminating between oceanic and non-oceanic basalts. – Earth Planet. Sci. Lett., **24**, 419–426, Amsterdam.

PICKERING, T.T., HISCOTT, R.N. & HEIN, F.J. (1989): Deep Marine Environments. Clastic Sedimentation and Tectonics. – 416 p, London (Unwin Hyman).

PRICE, W.J. (1979): Spectrochemical Analysis by Atomic Absorption. – 392 p., London (Heyden).

PROHASKA, W. & EBNER, F. (1988): Geochemische Untersuchungen an Metavulkaniten der Veitscher Decke/ Grauwackenzone. – Sber. Österr. Akad. Wiss., math.-naturw. Kl., Abt. I, **197**, 191–205, Wien.

ROCK, N.M.S. & LEAKE, B.E. (1984): The international mineralogical association amphibole nomenclature scheme: computerization and its consquences. – Mineral. Mag., **48**, 211–227, London.

SCHÖNLAUB, H.P. (1973): Zur Kenntnis des Nord–Süd-Profiles im Nötschgraben westlich Villach. – Verh. Geol. B.-A., **1973**, 359–365, Wien.

SCHÖNLAUB, H.P.. (1982): Das Karbon von Nötsch. – In: Erläuterungen zu Blatt 200 Arnoldstein, 24–25, Wien (Geol. B.-A.).

SCHÖNLAUB, H.P.. (1985): Das Karbon von Nötsch und sein Rahmen. – Jb. Geol. B.-A. **127**/4, 673–692, Wien.

SHANMUGAM, G. & MOIOLA, R.J. (1988): Submarine Fans: Characteristics, Models, Classification, and Reservoir Potential. – Earth-Science Reviews, **24**, 383–428, Amsterdam.

SMITH, A.G. (1981): Phanerozoic equal-area maps. – Geol. Rundsch., **70**(1), 91–127, Stuttgart.

STOW, D.A.V. (1985): Brae Oilfield Turbidite System, North Sea. – In: BOUMA, A.H., NORMART, W.R. & BARNES, N.E. (Eds.) (1985): Submarine Fans and Related Turbidite Systems. – 231–236, New York (Springer).

SURLYK, F. (1978): Submarine fan sedimentation along fault scarps on tilted fault blocks (Jurassic-Cretaceous boundary, East Greenland). – Gronlands Geologiske Undersogelse, Bulletin **128**, 1–108, Kopenhagen.

SURLYK, F. (1984): Fan-Delta to Submarine Fan Conglomerates of the Volgian-Valanginian Wollaston Forland Group, East Greenland. – In: KOSTER, E.H. & STEEL, R.J. (Eds.): Sedimentology of Gravels and Conglomerates, Can. Soc. Petrol. Geol., Memoir **10**, 359–382, Calgary.

TEICH, T. (1982): Zum Chemismus der Badstubbrekzie im Unterkarbon von Nötsch in Kärnten. – Carinthia II, **172**/92, 91–96, Klagenfurt.

TOLLMANN, A. (1977): Geologie von Österreich, Bd. I. Die Zentralalpen. – 766 p., Wien (F. Deuticke).

TURNER, F.J. & VERHOOGEN, J. (1960): Igneous and Metamorphic Petrology. – New York (McGraw Hill).

VAI, G.B. (1976): Stratigrafia e paleogeografia ercinica delle Alpi. – Mem Soc. Geol. Ital., **13**, 7–37, Roma.

VAI, G.B. (1979): Tracing the Hercynian structural zones across "Neo-Europa": an introduction. – Mem. Soc. Geol. Ital., **20**, 39–45, Roma.

VAI, G.B. & COCOZZA, T. (1986): Tentative schematic zonation of the Hercynian chain in Italy. – Bull. Soc. geol. France, **1986** (8), t. II, no 1, 95–114, Paris.

VAN DER VOO, R. (1982): Pre-Mesozoic Paleomagnetism and Plate Tectonics. – Ann. Rev. Earth. Planet. Sci., **10**, 191–220, Amsterdam.

WAGNER, L.R. (1960): The major element variation of the layered series of the Skaergaard intrusion and a re-estimation of the average composition of the hidden layered series and of the successive residual magmas. – J. Petrol., 1, 364–398, Oxford.

WALKER, R.G. (1975): Generalized facies models for resedimented conglomerates of turbidite association. – Geol. Soc. Am. Bull., **86**, 737–748, Boulder.

WALKER, R.G. (1977): Deposition of upper Mesozoic resedimented conglomerates and associated turbidites in southwestern Oregon. – Geol. Soc. America Bull., **88**, 273–285, Boulder.

WALKER, R.G. (1978): Deep water sandstone facies and ancient submarine fans: models for exploration for stratigraphic traps. – Am. Ass. Petrol. Geol. Bull., **62**, 932–966, Tulsa.

WALKER, R.G. (1984): Turbidites and associated coarse clastic deposits. – In: WALKER, R.G. (Ed.): Facies Models (2nd Ed.), Geoscience Canada, Reprint Series, **1**, 171–188, Toronto.

WINCHESTER, J.A. & FLOYD, P.A. (1976): Geochemical magma type discrimination application to altered and metamorphosed basic igneous rocks. – Earth Planet. Sci. Lett., **28**, 459–469, Amsterdam.

WINCHESTER, J.A. & FLOYD, P.A. (1977): Geochemical discrimination of different magma series and their differentiation products using immobile elements. – Chem. Geol., **20**, 325–343, Amsterdam.

ZIEGLER, P.A. (1982): Geological Atlas of Western and Central Europe. – 130 p., Amsterdam (Elsevier).

ZIEGLER, P.A. (1984): Caledonian and Hercynian crustal consolidation of Western and Central Europe – a working hypothesis. – Geol. Mijnbouw, **63**(1), 93–108, Amsterdam.

ZIEGLER, P.A. (1986): Geodynamic model for the Paleozoic crustal consolidation of Western and Central Europe. – Tectonophysics, **126**, 303–328, Amsterdam.

Manuskript bei der Schriftleitung eingelangt am 25. November 1990.